ChemComm

Cite this: *Chem. Commun.*, 2012, **48**, 10856–10858

www.rsc.org/chemcomm

COMMUNICATION

A microporous lanthanide-tricarboxylate framework with the potential for purification of natural gas†

Yabing He,*[a] Shengchang Xiang,[b] Zhangjing Zhang,[b] Shunshun Xiong,[a] Frank R. Fronczek,[c] Rajamani Krishna,*[d] Michael O'Keeffe[e] and Banglin Chen*[a]

Received 7th August 2012, Accepted 11th September 2012
DOI: 10.1039/c2cc35729a

A novel robust three-dimensional lanthanide organic framework with high thermal stability has been demonstrated to exhibit the potential for purification of natural gas in nearly pure form from an 8-component gas mixture at room temperature.

There is an escalating interest in the design and synthesis of lanthanide metal–organic frameworks (Ln-MOFs) due to their intrinsic porosity characteristics and physical properties coming from the lanthanide ions. So far, research on Ln-MOFs has mainly been focused on photoluminescent properties,[1] while the construction of robust porous Ln-MOFs and their potential application in gas adsorption have been much less developed (Table S3, ESI†).[2,3] This is mainly because of the difficulty in constructing porous Ln-MOFs: the large coordination sphere and flexible coordination geometry of lanthanide ions lead to the formation of either condensed frameworks or only "structurally porous" frameworks which are readily collapsed once the terminal and free solvent molecules are removed during the activation. One of efficient strategies to construct robust porous lanthanide organic frameworks is to utilize rod-shaped secondary building units.[3]

Natural gas separation is a very important industrial process. Recent progress has shown that porous MOFs are very promising materials for separation of hydrocarbons; however, research has only been focused on 2–4 component separation.[4] Given the fact that the higher coordination numbers of the lanthanide ions (exemplified here by Yb^{3+}) and the bulky naphthalene groups in the designed ligand (H_3L, Scheme 1) will favor the formation of moderately porous MOFs, we herein report a porous Yb-MOF [Yb(L)]·3DMA (**UTSA-30**). This framework not only exhibits a novel (3,7)-coordinated rod structure; but more importantly is the first porous MOF for separation of methane in nearly pure form from an 8-component gas mixture at room temperature.

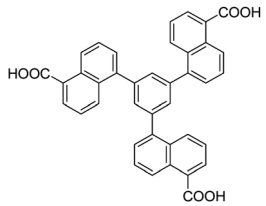

Scheme 1 The organic linker H_3L used to construct **UTSA-30**.

The organic linker H_3L was readily synthesized by a Pd-catalyzed Suzuki coupling between 1,3,5-tribromobenzene and methyl 6-(pinacolboryl)-2-naphthalate followed by base-catalyzed hydrolysis. A solvothermal reaction between H_3L and $Yb(NO_3)_3 \cdot 5H_2O$ in *N*,*N*′-dimethylacetamide (DMA) at 110 °C afforded small block-shaped colorless crystals of **UTSA-30**. The formula was established on the basis of single-crystal X-ray diffraction studies, thermogravimetric analysis (TGA), and microanalysis. The powder X-ray diffraction (PXRD) pattern of the bulk material is in good agreement with the simulated one (Fig. S1, ESI†), confirming the phase purity of the as-synthesized product. TGA under a nitrogen atmosphere shows an initial weight loss of 25.5% up to 165 °C, corresponding to the liberation of three free DMA molecules (calcd: 25.6%), followed by a wide plateau region until 420 °C, where the solid starts to decompose (Fig. S2, ESI†).

Single-crystal X-ray structure analysis reveals that **UTSA-30** adopts a three-dimensional (3D) framework which crystallizes in the trigonal space group $P\bar{3}m1$.‡ There are two crystallographically independent Yb atoms, which are, respectively, located on the Wyckoff positions 1a (0, 0, 0) and 1b (0, 0, 0.5) with $\bar{3}m$ symmetry. Each Yb atom is coordinated in an octahedral geometry by six carboxylate oxygen atoms from six different L ligands, whose naphthalene rings are disordered. The adjacent Yb^{3+} ions are bridged by three carboxylate groups from L ligands in a bis-monodentate *syn–syn* fashion (μ_2-$\eta1$:$\eta1$) to form infinite one-dimensional chains along the *c* axis (Fig. 1a). These chains are further interconnected by L ligands to construct a 3D

[a] *Department of Chemistry, University of Texas at San Antonio, One UTSA Circle, San Antonio, Texas 78249-0698, USA. E-mail: Yabing.He@utsa.edu, Banglin.Chen@utsa.edu; Fax: +1-210-458-7428*
[b] *Fujian Provincial Key Laboratory of Polymer Materials, Fujian Normal University, 3 Shangsan Road, Cangshang Region, Fuzhou 350007, China*
[c] *Department of Chemistry, Louisiana State University, Baton Rouge, LA 70803-1804, USA*
[d] *Van't Hoff Institute for Molecular Sciences, University of Amsterdam, Science Park 904, 1098 XH Amsterdam, The Netherlands. E-mail: r.krishna@uva.nl*
[e] *Department of Chemistry and Biochemistry, Arizona State University, Tempe, Arizona 85287, USA*

† Electronic supplementary information (ESI) available: Synthesis and characterization of the organic linker H_3L and **UTSA-30**, NMR, PXRD, TGA, FTIR, gas sorption isotherms, isotherm fitting parameters, calculations of the isosteric heats of adsorption, and the methodology for pulse chromatographic simulations. CCDC 894905. For ESI and crystallographic data in CIF or other electronic format see DOI: 10.1039/c2cc35729a

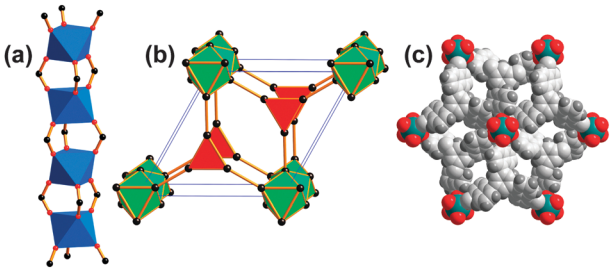

Fig. 1 X-ray single-crystal structure of **UTSA-30** indicating (a) one-dimensional rod $[Yb(CO_2)_3]_n$ as the infinite SBU, (b) (3,7)-coordinated net with RCSR symbol **hyb**, and (c) one-dimensional micropore along the *c* axis.

noninterpenetrated network. The resultant network contains one-dimensional tetragonal channels along the *c* axis (Fig. 1c). The calculation using PLATON[5] suggests that the 3D porous architecture has a solvent-accessible void volume of 30.3% after removing the guest molecules. It is noteworthy that **UTSA-30** is one of the very few Ln–MOFs in which the lanthanide center has a coordination number of 6 and no additional solvent molecule is attached to the Yb atoms to fulfill the usually high coordination numbers inherent to the lanthanide ions.[6]

As discussed by Rosi *et al.*[3] and by O'Keeffe and Yaghi,[7a] rod nets are best abstracted by taking the envelope of the points of extension (in this case the carboxylate carbon atoms). As shown in Fig. S3 (ESI),† these points form columns of face-sharing octahedra. A number of MOFs with such rods have been identified but all have been joined by ditopic linkers.[7a,c] We believe this is the first example in which such rods are joined by tritopic linkers. The underlying net is a simple (3,7)-coordinated net with RCSR symbol **hyb** with symmetry $P6_3/mmc$ (Fig. 1b).[7b]

The permanent porosity of the desolvated **UTSA-30a** was confirmed by gas sorption. **UTSA-30a** was generated by outgassing the acetone-exchanged **UTSA-30** under high vacuum at room temperature. The PXRD pattern matches with that of the pristine sample, indicating that the structure remains intact after removal of the solvent molecules. The N_2 sorption isotherm at 77 K displays reversible Type-I sorption behavior characteristic of microporous materials with Brunauer–Emmett–Teller (BET) and Langmuir surface areas of 592 and 604 $m^2\ g^{-1}$, respectively, and a pore volume of 0.259 $cm^3\ g^{-1}$.

Establishment of permanent microporosity and high thermal stability prompts us to examine its utility as an adsorbent for purifying natural gas. Natural gas, whose major component is methane, also contains a variety of undesirable impurities such as CO_2 and N_2 along with higher hydrocarbons such as C_2 and C_3 hydrocarbons. For use as a fuel, these components need to be separated to meet pipeline specifications. Accordingly, these gas sorption isotherms were measured. As shown in Fig. 2, the pure-component adsorption loadings follow the hierarchy: C_3 hydrocarbons (C_3H_6, C_3H_8) > C_2 hydrocarbons (C_2H_2, C_2H_4, C_2H_6) > CO_2 > CH_4 > N_2 (Fig. S7 and S8, ESI†). In addition, the isosteric heats of adsorption of these gases in **UTSA-30a**, which reflect their binding energies, also follow the same trend (Fig. S9, ESI†). These data indicate that it is possible to recover pure methane from a mixture containing a wide variety of impurities such as C_2H_2, C_2H_4, C_2H_6, C_3H_6, C_3H_8, CO_2, and N_2.

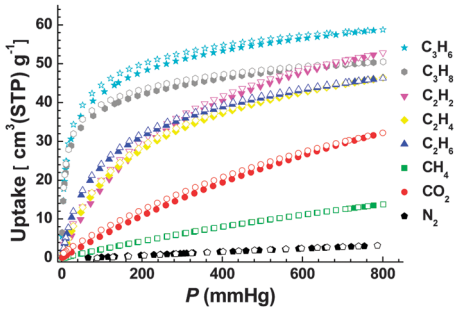

Fig. 2 The pure-component sorption isotherms for **UTSA-30a** at 296 K. Solid symbols: adsorption, open symbols: desorption.

In order to establish the feasibility of this separation, we performed calculations using the Ideal Adsorbed Solution Theory (IAST) of Myers and Prausnitz.[8] The validity of IAST estimations of CO_2–CH_4, CO_2–H_2, CH_4–H_2, and CO_2–N_2 mixture equilibria in a variety of MOFs (**MgMOF-74**, **MOF-177**, **BTP-COF**) and zeolites (**FAU**, **LTA**, **MFI**, **CHA**) has been established in earlier publications by comparison of IAST calculations with molecular simulations of binary adsorption equilibrium.[9] Fig. S10 (ESI†) presents IAST calculations of the component loadings for CH_4, C_2H_2, C_2H_4, C_2H_6, C_3H_6, C_3H_8, CO_2, and N_2 in an equimolar 8-component mixture as a function of the total bulk gas phase pressure at 296 K. The IAST calculations show that the component loadings in the mixture are grouped into five different sub-groups with the following loading hierarchies: C_3 hydrocarbons (C_3H_6, C_3H_8) > C_2 hydrocarbons (C_2H_2, C_2H_4, C_2H_6) > CO_2 > CH_4 > N_2. Fig. 3 presents calculations of the four different adsorption selectivities: (C_3H_6 + C_3H_8)/(C_2H_2 + C_2H_4 + C_2H_6), (C_2H_6 + C_2H_4 + C_2H_2)/CH_4, CO_2/CH_4, and CH_4/N_2, as a function of the total bulk gas phase pressure at 296 K. All four selectivities are in excess of about 2, indicating that fairly sharp separations can be achieved of the 8-component mixture to obtain five different fractions. The CH_4/N_2 selectivity is about five, and exceeds that of traditionally used adsorbents such as **MFI** and **NaX** zeolites.[10]

To further demonstrate the feasibility of using **UTSA-30a** for natural gas purification, we performed pulse chromatographic simulations following the methodologies developed and described in earlier works.[9e,11] Experimental validation of the chromatographic simulation methodology is provided in earlier works.[9e,11c,12] Fig. 4 shows the pulse chromatographic separation of an equimolar

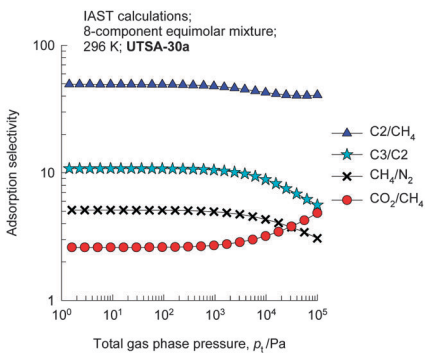

Fig. 3 IAST calculations of (C_3H_6 + C_3H_8)/(C_2H_2 + C_2H_4 + C_2H_6), (C_2H_6 + C_2H_4 + C_2H_2)/CH_4, CO_2/CH_4, and CH_4/N_2 adsorption selectivities as a function of the total bulk gas phase pressure at 296 K.

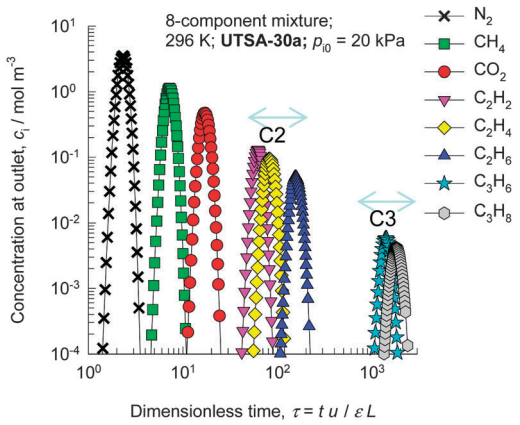

Fig. 4 Pulse chromatographic separation of an equimolar 8-component mixture CH_4–CO_2–N_2–C_2H_2–C_2H_4–C_2H_6–C_3H_6–C_3H_8 using **UTSA-30a** at 296 K. The *x*-axis is the dimensionless time. The pulse of the equimolar mixture, with partial pressures of 20 kPa each, is injected for 10 s at the start of the process, and subsequently the adsorbed components are desorbed by use of purge inert gas.

8-component CH_4–CO_2–N_2–C_2H_2–C_2H_4–C_2H_6–C_3H_6–C_3H_8 mixture with **UTSA-30a** at 296 K. The first peak to emerge from the adsorber is that of N_2 which can be recovered in nearly pure form. Following the removal of N_2, we see the emergence of the peak for CH_4 that can be recovered in pure form, practically free of impurities. The next peak to emerge from the adsorber is that of CO_2, which can be recovered and perhaps sequestered. Following the removal of CO_2, we note that the next set of peaks are for the C_2 hydrocarbons (C_2H_6 + C_2H_4 + C_2H_2). **UTSA-30a** is not able to separate these into individual components. Once the C_2 hydrocarbons are collected, these can be separated into nearly pure components by use of adsorbents such as **MgMOF-74** and **FeMOF-74**.[11c,12] The last set of peaks to emerge are those of C_3 hydrocarbons (C_3H_6 + C_3H_8). Once the C_3 hydrocarbon mixtures are collected, these can be separated to produce polymer-grade C_3H_6 by use of adsorbents such as **MgMOF-74** and **FeMOF-74**.[11c,12]

The influence of the composition of the feed gas on the performance of **UTSA-30a** was also investigated in detail. These results are presented in Fig. S11 and S13 (ESI†). The adsorption selectivities are not significantly influenced by mixture compositions, and the fractionation ability is not dependent on the chosen mixture composition. By comparison, the separation performance of **UTSA-30a** for purification of natural gas is comparable to that of the traditionally used **NaX** zeolite, as evidenced from Fig. S14 (ESI†). There are no strong binding sites to interact with hydrocarbons, so both pore sizes and curvatures have played the important roles in hydrocarbon separation.

In summary, a robust porous Ln-MOF with high thermal stability and novel topology was constructed from a new aromatic tricarboxylate, exhibiting the potential for separation of carbon dioxide, nitrogen, and heavy hydrocarbons from methane for natural gas purification purpose. It is expected that this work will initiate more investigations on the emerging MOFs for such an industrially important separation.

This work was supported by an AX-1730 from Welch Foundation (BC), and partially supported by NSFC (21273033, 21203024) and the Award 'Min-Jiang Scholar Program' in Fujian Province, China.

Notes and references

‡ Crystal data for **UTSA-30**: $C_{51}H_{48}N_3O_9Yb$, M = 1019.98, trigonal, space group $P\bar{3}m1$, a = b = 17.0600(17) Å, c = 9.2376(18) Å, V = 2328.3(6) Å^3, Z = 2, D_c = 1.455 g cm^{-3}, μ(Mo-K$_\alpha$) = 2.067 mm^{-1}, F(000) = 1034, final R_1 = 0.0496 for $I > 2\sigma(I)$, wR_2 = 0.1722 for all data, GoF = 1.072, CCDC 894905.

1 (*a*) P. Falcaro and S. Furukawa, *Angew. Chem., Int. Ed.*, 2012, **51**, 8431; (*b*) Y. Cui, H. Xu, Y. Yue, Z. Guo, J. Yu, Z. Chen, J. Gao, Y. Yang, G. Qian and B. Chen, *J. Am. Chem. Soc.*, 2012, **134**, 3979; (*c*) B. Chen, S. Xiang and G. Qian, *Acc. Chem. Res.*, 2010, **43**, 1115; (*d*) Y. Cui, Y. Yue, G. Qian and B. Chen, *Chem. Rev.*, 2012, **112**, 1126.

2 (*a*) T. M. Reineke, M. Eddaoudi, M. O'Keeffe and O. M. Yaghi, *Angew. Chem., Int. Ed.*, 1999, **38**, 2590; (*b*) L. Pan, K. M. Adams, H. E. Hernandez, X. Wang, C. Zheng, Y. Hattori and K. Kaneko, *J. Am. Chem. Soc.*, 2003, **125**, 3062; (*c*) T. Devic, C. Serre, N. Audebrand, J. Marrot and G. Férey, *J. Am. Chem. Soc.*, 2005, **127**, 12788; (*d*) T. K. Maji, G. Mostafa, H.-C. Chang and S. Kitagawa, *Chem. Commun.*, 2005, 2436; (*e*) J. Jia, X. Lin, A. J. Blake, N. R. Champness, P. Hubberstey, L. Shao, G. Walker, C. Wilson and M. Schröder, *Inorg. Chem.*, 2006, **45**, 8838; (*f*) Y. K. Park, S. B. Choi, H. Kim, K. Kim, B.-H. Won, K. Choi, J.-S. Choi, W.-S. Ahn, N. Won, S. Kim, D. H. Jung, S.-H. Choi, G.-H. Kim, S.-S. Cha, Y. H. Jhon, J. K. Yang and J. Kim, *Angew. Chem., Int. Ed.*, 2007, **46**, 8230; (*g*) S. Ma, X.-S. Wang, D. Yuan and H.-C. Zhou, *Angew. Chem., Int. Ed.*, 2008, **47**, 4130; (*h*) H.-L. Jiang, N. Tsumori and Q. Xu, *Inorg. Chem.*, 2010, **49**, 10001; (*i*) L.-H. Xie, Y. Wang, X.-M. Liu, J.-B. Lin, J.-P. Zhang and X.-M. Chen, *CrystEngComm*, 2011, **13**, 5849.

3 N. L. Rosi, J. Kim, M. Eddaoudi, B. Chen, M. O'Keeffe and O. M. Yaghi, *J. Am. Chem. Soc.*, 2005, **127**, 1504.

4 (*a*) Y. He, Z. Zhang, S. Xiang, H. Wu, F. R. Fronczek, W. Zhou, R. Krishna, M. O'Keeffe and B. Chen, *Chem.–Eur. J.*, 2012, **18**, 1901; (*b*) Y. He, Z. Zhang, S. Xiang, F. R. Fronczek, R. Krishna and B. Chen, *Chem.–Eur. J.*, 2012, **18**, 613; (*c*) M. C. Das, H. Xu, S. Xiang, Z. Zhang, H. D. Arman, G. Qian and B. Chen, *Chem.–Eur. J.*, 2011, **17**, 7817; (*d*) Y. He, Z. Zhang, S. Xiang, F. R. Fronczek, R. Krishna and B. Chen, *Chem. Commun.*, 2012, **48**, 6493; (*e*) S. Xiang, Z. Zhang, C.-G. Zhao, K. Hong, X. Zhao, D.-L. Ding, M.-H. Xie, C.-D. Wu, R. Gill, K. M. Thomas and B. Chen, *Nat. Commun.*, 2011, **2**, 204.

5 A. L. Spek, *J. Appl. Crystallogr.*, 2003, **36**, 7–13; A. L. Spek, *PLATON, A Multipurpose Crystallographic Tool*, Utrecht University, The Netherlands, 2006.

6 D. T. d. Lill and C. L. Cahill, *Chem. Commun.*, 2006, 4946.

7 (*a*) M. O'Keeffe and O. M. Yaghi, *Chem. Rev.*, 2012, **112**, 675; (*b*) M. O'Keeffe, M. A. Peskov, S. J. Ramsden and O. M. Yaghi, *Acc. Chem. Res.*, 2008, **41**, 1782; (*c*) Z. Yan, M. Li, H.-L. Gao, X.-C. Huang and D. Li, *Chem. Commun.*, 2012, **48**, 3960.

8 A. L. Myers and J. M. Prausnitz, *AIChE J.*, 1965, **11**, 121.

9 (*a*) Z. R. Herm, J. A. Swisher, B. Smit, R. Krishna and J. R. Long, *J. Am. Chem. Soc.*, 2011, **133**, 5664; (*b*) R. Krishna and J. M. van Baten, *J. Membr. Sci.*, 2011, **377**, 249; (*c*) R. Krishna and J. M. van Baten, *Phys. Chem. Chem. Phys.*, 2011, **13**, 10593; (*d*) R. Krishna and J. M. van Baten, *J. Membr. Sci.*, 2011, **383**, 289; (*e*) H. Wu, K. Yao, Y. Zhu, B. Li, Z. Shi, R. Krishna and J. Li, *J. Phys. Chem. C*, 2012, **116**, 16609.

10 V. P. Mulgundmath, F. H. Tezel, F. Hou and T. C. Golden, *J. Porous Mater.*, 2012, **19**, 455.

11 (*a*) R. Krishna and J. R. Long, *J. Phys. Chem. C*, 2011, **115**, 12941; (*b*) R. Krishna and J. M. van Baten, *Sep. Purif. Technol.*, 2012, **87**, 120; (*c*) Y. He, R. Krishna and B. Chen, *Energy Environ. Sci*, 2012, **5**, 9107.

12 E. D. Bloch, W. L. Queen, R. Krishna, J. M. Zadrozny, C. M. Brown and J. R. Long, *Science*, 2012, **335**, 1606.